PACS 61.30.Gd, 47.54.-r, 64.70.M-

Defect dynamics in roll structures of twisted nematics

V. A. Delev†, E. S. Batyrshin, O. A. Scaldin, Yu. A. Lebedev, Yu I. Timirov

†delev@anrb.ru

Institute of Molecule and Crystal Physics URC RAS, Oktyabrya Av. 151, 450075 Ufa, Russia

At application of ac voltage exceeding some critical value $U \geq U_c$ to the twisted at π/2 nematic liquid crystal (NLC) sandwiched between transparent electrodes the electroconvective instability is occurred. So that, a periodic roll system is formed, with the rolls axes oriented normally to the initial molecule orientation (so-called director *n*) in the middle of NLC layer. The distinctive feature of this roll system is a presence of an helical hydrodynamic flows with the opposite direction in the neighboring rolls in addition to the convective (tangential) component of the velocity of the hydrodynamic flow. An arising electroconvective domain structure is usually accompanied by the generation of very diverse defects, which is stationary near the threshold voltage. Among them there exist ordinary singular dislocations as well as nonsingular defects. Of particular interest are the defects with the nonsingular core, which are not observed in the NLCs with the uniform molecule orientation, as well defects with core dissociated in line (so-called «extended core»). Above threshold voltage all defects in domain structure begin to oscillate. Such oscillations are periodic closures and openings of co-aligned axial components of the velocity of the hydrodynamic flow in rolls located on both sides of the defect core (or "zig-zag" oscillation).The specific features of oscillation dynamics of singular and nonsingular defects above threshold voltage have been revealed. It has been found that the average frequency of the "zig-zag" oscillation depends on the defect core size and applied voltage. It slightly decreases with defect core growth and almost linearly increases with voltage. For both singular and nonsingular defects the marked asymmetry in their space-temporal dynamics has been observed. The origin of similar asymmetry has established to be connected with clockwise or counterclockwise direction of director *n* turn at twisted NLC cell preparation stage.

Keywords: electroconvection, nematic liquid crystal, domain structure, defects.

1. Introduction

Nematic liquid crystal (NLC) is an anisotropic liquid with a low conductivity characterized by orientation ordering of the elongated molecules. Preferred direction of NLC molecules orientation is described by the director field ***n*** [1]. Electroconvection appears when voltage exceeding some critical value $U \geq U_c$ is applied to NLC layer between the conducting substrates. This being the case, a periodic roll system is formed, with the rolls axes oriented normally to the initial orientation of the director ***n***. Depending on NLC material parameters, boundary conditions and applied voltage parameters, electroconvection system demonstrates a unique variety of modulated structures [1, 2]. Besides, scenarios of structure transformations in NLC electroconvection system essentially depend on availability in domain structure of defects and flexoelectric effect development [2-4].

Dynamics and statistic characteristics of singular defects in roll structures at electroconvection in NLC were classified and studied thoroughly for homogeneous border conditions [5-7]. In more complicated situation, e.g. in quasi-one-dimensional twisted NLC, the linear local formations with phase jump along them on π [8, 9] were discovered.

But the dynamics of defects in NLC electroconvection system with the non-homogeneous director ***n*** field distribution still remains under investigation [10, 11]. That's why this work is aimed to study the peculiarities of defects dynamics in roll structure in π/2 twisted NLC in alternating electrical field.

2. Materials and experimental techniques

4-n-methoxybenziliden-n-butylaniline (MBBA) was used as NLC, it was placed in a liquid crystal cell between two glass substrates with a conductive transparent coating of SnO_2, separated by a mica film of d=20±2 μm thickness. Transparent electrodes were covered with a polymer layer (*Polyimide*), which was rubbed in one direction to create a homogeneous planar orientation of the director n. Then they were turned to π/2 to create a twisted configuration of the director field in the NLC layer (figure 1a). In this case, at the bottom substrate the director orientation $\boldsymbol{n}_1$ is orthogonal to the top substrate director orientation $\boldsymbol{n}_2$.

Alternating voltage $U=U_a \sin(2\pi ft)$ with frequency f=30 Hz was applied to the NLC layer. The threshold voltage of roll structure is U_c=5,6 V.

Domain structures and their defects were observed in a polarization microscope Axiolab (Zeiss, Germany), their images were registered by video camera with resolution 1024×1024 pixels and 256 gradations of the grey colour.

3. Results and discussion

The images of electroconvection structures are space periodic modulations of the intensity of light passed through the NLC cell. These modulations correspond to different modes induced by the external electric field in the system. At the threshold of electroconvection the hydrodynamic vortex modes (rolls) are induced and form images shaped like the dark and light stripes (figure 1b). As one can see from the figure 1b, the roll structure is characterized by a large number of various defects.

Elementary singular defect (dislocation) formed in the roll structure of twisted NLC is an additional (or deficient) pair of rolls arising during a counter-clockwise contour pass around the defect core [9].

It is necessary to underline that though above mentioned defects do not make *"zig-zag"* oscillations near the threshold, they drift slowly along the rolls throughout the system. That is why the defects which do not oscillate are called stationary ones. Opposite signed defects annihilate when interact.

In contrast to the planar oriented NLC, along with edge dislocations having topological charge $S=\pm1$ (fig. 2a) the following defects are found in twisted nematics above the threshold: dislocations with spread (or dissociated) core with $S=\pm1$ (figure 2b) and nonsingular defects with topological charge $S=0$ of different size (figure 2c,d).

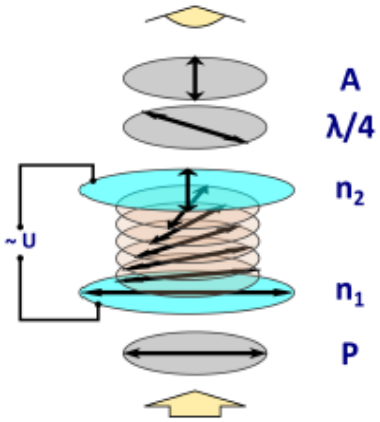

(a)

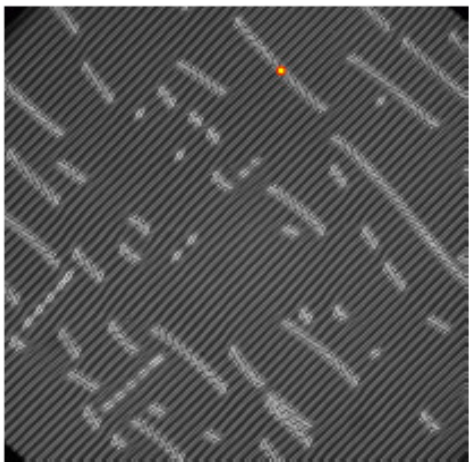

(b)

Fig. 1. Optic scheme of experiment (a) for observation of electroconvection structures ($U=1{,}6U_c$ B) and their defects in π/2 twisted NLC (b).

Figure 2c,d shows the same number of rolls above and below the border that corresponds to zero topological charge $S=0$. Nonsingular defects are caused by large-scale spatial fluctuations of orientation and hydrodynamic system mode («localized phase modulation») [6]. These defects exist only due to axial component of NLC hydrodynamic flow velocity $\mathbf{v}_a$ in rolls which has opposite directions in adjacent rolls (figure 2c) [12].

Nonsingular defect is a boundary (or domain wall) without hydrodynamic flow through it. In this case flow is continuous due to its locking in adjacent rolls on one side of domain wall, so that near its border the flow direction is changed to opposite one (fig. 2a,c). The rolls located above the defect are displaced from the ones located below the defect core for about a half of the spatial period λ (fig.1b). Minimum size of nonsingular defect L is equal to the size of roll structure elementary cell $L_{min}=2\lambda$, where λ is the lateral dimension of one roll, i.e. this is one pair of adjacent rolls with axial velocity opposite direction in them.

Nonsingular stationary defects of arbitrary discrete size 2λ, 4λ, 6λ, etc. can be seen near the threshold U_c. Figure 3 shows fine structures of oscillating singular and nonsingular defects.

Nonsingular elementary defects can be formed according to three scenarios: (i) spontaneously; (ii) as a result of interaction of two dislocations with charges +1 and -1; (iii) as a result of detachment from dislocation with a spread core.

Axial component of flow velocity $\mathbf{v}_a$ in rolls is increased [12] with the increase of the applied voltage U, as a result of these the pressure of hydrodynamic flow on domain wall is increased and the defect begins to make *"zig-zag"* oscillations. These oscillations are periodic closing and opening of the codirectional axial components of flow velocity.

Oscillations of a charged defect consist of a periodic formation of elementary dislocations with $S=-1$ either at the left defect edge (the first half of the oscillation period T_1) or at the right one (the second half of the period T_2). (Figure 3). During this process, the rolls in defect core are in a *"zig"* state (with rolls inclined to the right) at the end of period T_1 and in *"zag"* state (with rolls inclined to the left) upon T_2.

Similar *"zig-zag"* oscillations are carried out also by a nonsingular defect. But in this case a periodical simultaneous appearance of a pair of opposite charged elementary dislocations at the edges of the defect within T_1 period and followed by their annihilation upon T_2 completion (Figure 3, b) takes place.

Thus, the dynamics of oscillating defects can be represented as a periodical change of inclined rolls from *"zig"* to *"zag"* mode.

To determine the frequency of *"zig-zag"* oscillations of defects spatial demodulation technique has been applied to initial images [13], which allows one to exclude the normal rolls structure from initial images and to determine defects areas only.

Firstly, a direct 2-dimensional Fourier transform F of initial images $I(x, y)$ is done (Figure 4 – insert). In the Fourier

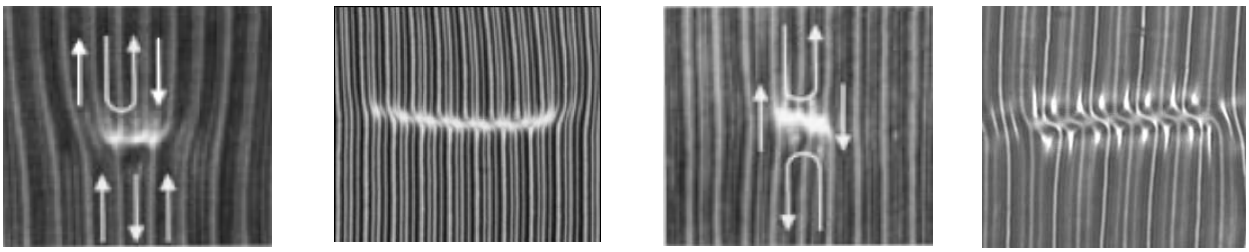

Fig. 2. Singular defects with *S*= -1: elementary defect (a) and dislocation with blur nucleus (b). Non singular defects with *S*=0 of various sizes *L*=2λ (c) и *L*=4λ (d).

image obtained a round mask is selected which corresponds to a *"zig"* and *"zag"* mode. The rest part of spectrum set to zero. Only one reflection (e.g. positive) is marked out in the spectrum. Absolute value of inverse Fourier transform evaluates the amplitude of appropriate mode:

$$A_{zig}(x, y)=|F^{-1}\{M_{zig}(X, Y)\cdot F[I(x, y)]\}|,$$

$$A_{zag}(x, y)=|F^{-1}\{M_{zag}(X, Y)\cdot F[I(x, y)]\}|,$$

where $M_{zig}(X, Y)$, $M_{zag}(X, Y)$ are binary masks, which cut a required reflection in spectrum; F and F^{-1} are operators of direct and inverse Fourier transform; $F[I(x, y)]$ is the Fourier transform of initial image. The masks were determined as follows:

$$M(X,Y)(t)=\begin{cases}1, \sqrt{(X-X_0)^2+(Y-Y_0)^2}\le R,\\ 0, \sqrt{(X-X_0)^2+(Y-Y_0)^2}> R,\end{cases}$$

where (X_0, Y_0) determine the center of required reflection, R was chosen to cover the mask completely. Intensity of images in defect areas increases considerably after applied demodulation technique and this allows one to determine the oscillation frequency more accurately and to study defect dynamic in details. Amplitude difference of *"zig"* and *"zag"* rolls $A_{zig}(x, y)-A_{zag}(x, y)$ gives the highest contrast.

Figure 5 shows the changes of local dynamics of intensity for the light modulated by *"zig-zag"* oscillations in the defect area before and after demodulation.

It should be noted that for both types of defects, singular and nonsingular, asymmetry of spatiotemporal dynamics is found, i.e. $T_1 \neq T_2$, namely $T_1 > T_2$ [9]. It is established that this asymmetry is definitely connected with twist direction of director field ***n***, which appears at the stage of LC cell formation, when the top substrate turns around the bottom one, i.e clockwise or counter-clockwise.

Linear defects appear slightly above the electroconvection threshold U_c, and their *"zig-zag"* oscillations are registered only at $U \approx 7{,}8$ V (fig. 6) and can be observed up to the dynamic scattering regime, but the frequency scatter (the Fourier spectrum width) is increased considerably.

To reveal the relation between average defects oscillations frequency $\langle f \rangle$ and its length *L*, ten video sequences of 1024 shots were made, which allowed to collect statistics on dozens of defects (60÷100). This procedure allowed every time to get new defects in microscope field of view without LC sample displacement. Figure 7 shows the results for $U=1{,}6U_c$ B.

The dependence presented in figure 7 shows a decrease of average oscillation frequency $\langle f \rangle$ with the defect length

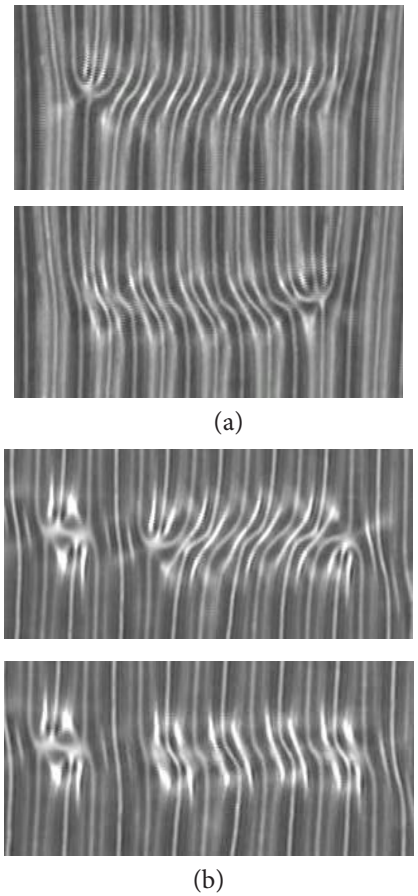

Fig. 3. Oscillating singular defect with *S*=-1 in dissociated dislocation core (a) and nonsingular ("breather") defects with *S*=0 after semi-period of oscillations. Here *"zig"* mode means inclination to the right (top) and *"zag"* mode is inclination to the left (bottom).

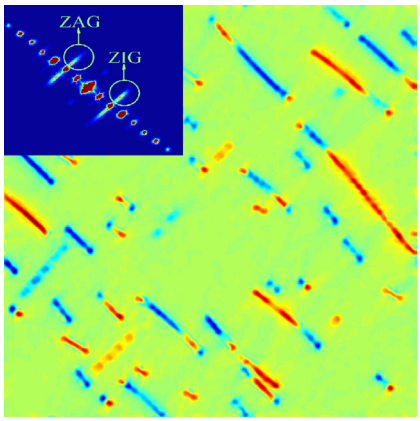

Fig. 4. Result of initial structure image demodulation (figure1b). Inserted is structure factor (squared module Fourier transform) of initial structure image.

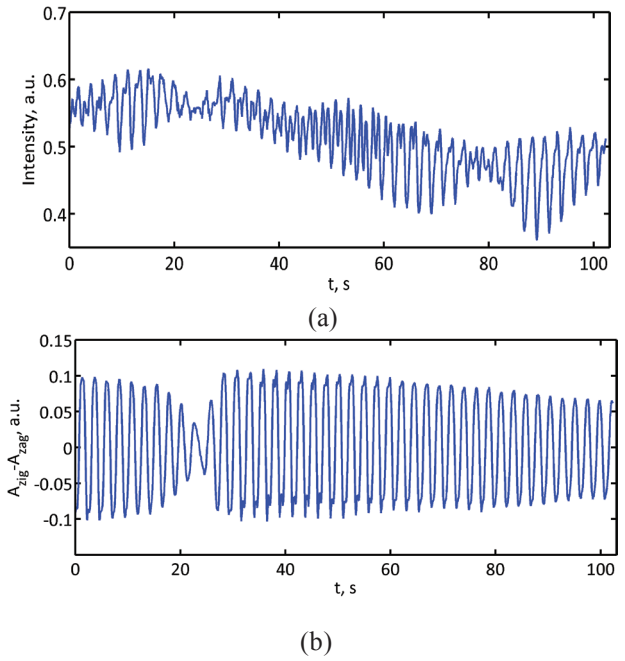

Fig. 5. Local dynamics of initial image intensity (a) and amplitude difference $A_{zig}(x, y)$–$A_{zag}(x, y)$ of inclined rolls in defect (b) at U=1,6U_c V.

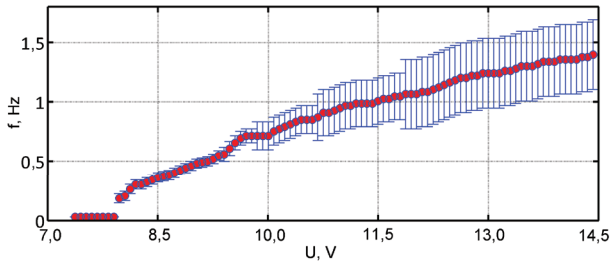

Fig. 6. Relation between frequency of "zig-zag" oscillations f of linear defect and applied voltage U.

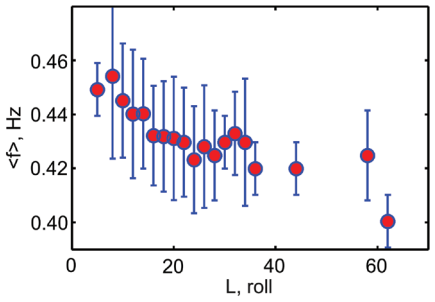

Fig. 7. Relation between average frequency of *"zig-zag"* oscillations <*f*> of linear defect and its length L at U=1,6U_c V.

L, though the errors of estimates are high. These errors are random in nature that manifests itself in the fact that shorter defects have a fairly wide scatter of frequency, while long ones have a low frequency as a rule.

4. Conclusions

This work described the features of defect dynamics in the roll structures, which appear in an electroconvection system of twisted NLC caused by alternating voltage. New defect types are demonstrated to form due to the axial component of velocity of hydrodynamic flow with opposite direction in the adjacent rolls. Assymetry in spatial-temporal dynamics is determined by direction of the director field ***n*** twisting in NLC layer at preparation stage.

Acknowledgements. The work is supported by RFBR, grants No. 13-02-01117 and 15-02-09366.

References

1. S.A. Pikin. Structural transitions in liquid crystals. Moskva, Nauka (1981) 336 p. (in Russian).
2. Pattern Formation in Liquid Crystals, ed. by Buka A., Kramer L., New York, Springer-Verlag (1996) 339 p.
3. T. Tóth-Katona, N. Éber, and Á. Buka. Mol. Cryst. Liq. Cryst. **511**, 11/1481 (2009).
4. E.S. Batyrshin, A.P. Krekhov, O.A. Skaldin, and V.A. Delev. JETP **114**(6), 1052 (2012).
5. S. Rasenat, V. Steinberg, I. Rehberg. Phys. Rev. A **42**, 5998 (1990).
6. A. Joets, R. Ribotta. J. Phys. (France) **47**, 595 (1986).
7. S. Kai, N. Chizumi, M. Kohno. J. Phys. Soc. Jap. **58**(10), 3541 (1989).
8. V.A. Delev, P. Toth, and A.P. Krekhov. Mol. Cryst. Liq. Cryst. **351**, 179 (2000).
9. O.A. Skaldin, G.R. Yakupova, V.A. Delev, Yu.A. Lebedev, A.A. Nazarov. Phys. of the Solid State **47**(2), 374 (2005).
10. O.A. Skaldin, V.A. Delev, E.S. Shikhovtseva, E.S. Batyrshin, Yu.A. Lebedev. JETP Letters **93**(7), 388 (2011).
11. O.A. Skaldin, V.A. Delev, E.S. Shikhovtseva. JETP Letters **97**(2), 92 (2013).
12. A. Hertrich, A.P. Krekhov, O.A. Scaldin. J. Phys. II (France) **4**, 239 (1994).
13. M. Scheuring, L. Kramer, J. Peinke. Phys. Rev. E **58**, 2018 (1998).